Article

Magnetoswitchable Reactions of DNA Monolayers on Electrodes: Gating the Processes by Hydrophobic Magnetic Nanoparticles

Eugenii Katz, Yossi Weizmann, and Itamar Willner

J. Am. Chem. Soc., **2005**, 127 (25), 9191-9200• DOI: 10.1021/ja0517771 • Publication Date (Web): 04 June 2005

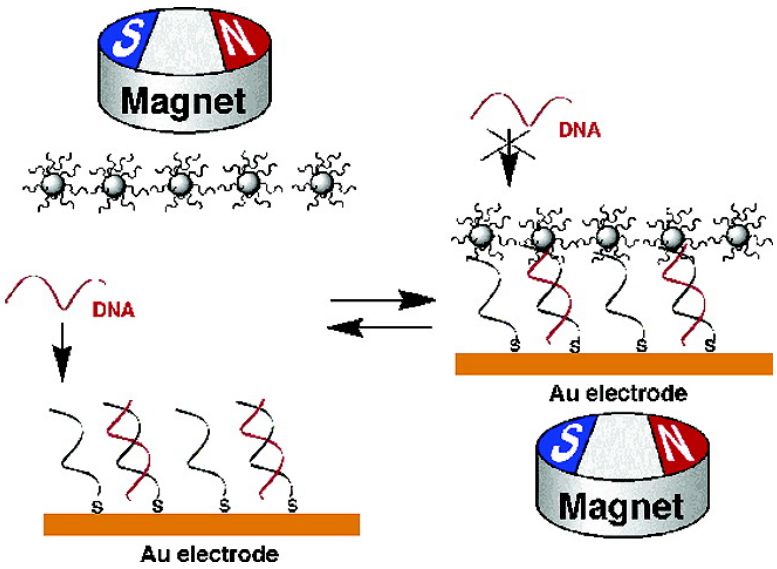

More About This Article

Additional resources and features associated with this article are available within the HTML version:

- Supporting Information
- Links to the 7 articles that cite this article, as of the time of this article download
- Access to high resolution figures
- Links to articles and content related to this article
- Copyright permission to reproduce figures and/or text from this article

View the Full Text HTML

J|A|C|S
ARTICLES
Published on Web 06/04/2005

Magnetoswitchable Reactions of DNA Monolayers on Electrodes: Gating the Processes by Hydrophobic Magnetic Nanoparticles

Eugenii Katz, Yossi Weizmann, and Itamar Willner*

Contribution from the Institute of Chemistry, The Hebrew University of Jerusalem, Jerusalem 91904, Israel

Received March 21, 2005; E-mail: willnea@vms.huji.ac.il

Abstract: Biorecognition and biocatalytic reactions of DNA monolayers, such as hybridization, polymerization, and hydrolytic digestion, were followed in situ by chronocoulometry and Faradaic impedance spectroscopy. Hydrophobic magnetic nanoparticles attracted to, and retracted from, the electrode surface by an external magnetic field were used to activate and inhibit the DNA-monolayer reactions, respectively. The attraction of the magnetic nanoparticles to the electrode surface generated a hydrophobic thin film on the surface that is not permeable for the water-soluble components required for the DNA-monolayer reactions. This results in the inhibition of the DNA-monolayer reactions. The retraction of the magnetic nanoparticles from the surface regenerated the free nucleic acid-functionalized surface that was exposed to the aqueous solution, thus reactivating the DNA-monolayer reactions. The reversible inhibition and activation of the DNA-monolayer reactions upon the cyclic attraction−retraction of the hydrophobic magnetic nanoparticles may be used to synthesize programmed DNA chips.

Introduction

Self-assembled monolayers of enzymes, antigens and antibodies, and oligonucleotides on electrodes were extensively studied and used to develop electrochemical enzyme-based biosensors,[1] immunosensors,[2] and DNA sensors.[3] Biomolecule-functionnalized electrode arrays were developed to allow parallel, high-throughput, multitarget analysis.[4] Reversible activation and inhibition of biocatalytic and biorecognition processes on electrode interfaces was achieved by the conjugation of switchable molecular units with the biomolecule-functionalized interfaces. For example, photoisomerizable molecules linked to electrode surfaces were employed as command interfaces[5] for controlling by light bioelectrocatalytic and biorecognition processes, and the systems led to the development of light-switchable biosensors[6] and immunosensors.[7]

Extensive research was recently directed to the synthesis of metallic, semiconductor, and magnetic nanoparticles coupled to biomolecules and to the use of the hybrid systems for electronic and optical biosensing, design of nanocircuitry, and the assembly of nanodevices.[8] Magnetic particles functionalized with redox mediators, cofactors, and enzymes were used to transport the active molecular components to and from the electrode surface by means of an external magnet, thus resulting in the reversible activation and inhibition of the bioelectrocatalytic processes on the electrode surfaces.[9]

Recently, we reported on the application of hydrophobic magnetic nanoparticles to control the interfacial properties of electrode surfaces by the reversible attraction and retraction of the nanoparticles to, and from, the electrode support by means of an external magnet.[10,11] The attraction of the hydrophobic magnetic nanoparticles to the electrode surface by an external magnet results in the formation of a hydrophobic thin film on the conductive support that yields a barrier for electrochemical

(1) (a) Willner, I.; Katz, E. *Angew. Chem., Int. Ed.* **2000**, *39*, 1180−1218. (b) Katz, E.; Shipway, A. N.; Willner, I. In *Encyclopedia of Electrochemistry*; Wilson, G. S., Bard, A. J., Stratmann, M., Eds.; Wiley-VCH: Weinheim, Germany, 2002; Vol. 9, Chapter 17, pp 559−626. (c) Schmidt, H.-L.; Schuhmann, W. *Biosens. Bioelectron.* **1996**, *11*, 127−135. (d) Habermüller, K.; Mosbach, M.; Schuhmann, W. *Fresenius' J. Anal. Chem.* **2000**, *366*, 560−568. (e) Armstrong, F. A.; Heering, H. A.; Hirst, J. *Chem. Soc. Rev.* **1997**, *26*, 169−179. (f) Armstrong, F. A.; Wilson, G. S. *Electrochim. Acta* **2000**, *45*, 2623−2645.

(2) (a) Rogers, K. R. *Mol. Biotechnol.* **2000**, *14*, 109−129. (b) Ivnitski, D.; Abdel-Hamid, I.; Atanasov, P.; Wilkins, E. *Biosens. Bioelectron.* **1999**, *14*, 599−624. (c) O'Sullivan, C. K.; Vaughan, R.; Guilbault, G. G. *Anal. Lett.* **1999**, *32*, 2353−2377.

(3) (a) Bardea, A.; Patolsky, F.; Dagan, A.; Willner, I. *Chem. Commun.* **1999**, 21−22. (b) Patolsky, F.; Katz, E.; Bardea, A.; Willner, I. *Langmuir* **1999**, *15*, 3703−3706. (c) Patolsky, F.; Ranjit, K. T.; Lichtenstein, A.; Willner, I. *Chem. Commun.* **2000**, 1025−1026. (d) Wang, J. *Anal. Chim. Acta* **2002**, *469*, 63−71. (e) Kerman, K.; Kobayashi, M.; Tamiya, E. *Meas. Sci. Technol.* **2004**, *15*, R1−R11.

(4) (a) Lee, B. H.; Nagamune, T. *Biotechnol. Bioprocess Eng.* **2004**, *9*, 69−75. (b) Bier, F. F.; Kleinjung, F. *Fresenius' J. Anal. Chem.* **2001**, *371*, 151−156.

(5) (a) Willner, I.; Willner, B. *Pure Appl. Chem.* **2001**, *73*, 535−542. (b) Katz, E.; Willner, B.; Willner, I. *Biosens. Bioelectron.* **1997**, *12*, 703−719. (c) Willner, I.; Willner, B. *J. Mater. Chem.* **1998**, *8*, 2543−2556.

(6) Willner, I.; Doron, A.; Katz, E. *J. Phys. Org. Chem.* **1998**, *11*, 546−560.

(7) (a) Willner, I.; Willner, B. *Biotechnol. Prog.* **1999**, *15*, 991−1002. (b) Patolsky, F.; Filanovsky, B.; Katz, E.; Willner, I. *J. Phys. Chem. B* **1998**, *102*, 10359−10367. (c) Blonder, R.; Levi, S.; Tao, G. L.; Ben-Dov, I.; Willner, I. *J. Am. Chem. Soc.* **1997**, *119*, 10467−10478. (d) Willner, I.; Blonder, R.; Dagan, A. *J. Am. Chem. Soc.* **1994**, *116*, 9365−9366.

(8) (a) Katz, E.; Willner, I. *Angew. Chem., Int. Ed.* **2004**, *43*, 6042−6108. (b) Niemeyer, C. M. *Angew. Chem., Int. Ed.* **2001**, *40*, 4128−4158.

(9) (a) Willner, I.; Katz, E. *Angew. Chem., Int. Ed.* **2003**, *42*, 4576−4588. (b) Katz, E.; Sheeney-Haj-Ichia, L.; Willner, I. *Chem.−Eur. J.* **2002**, *8*, 4138−4148. (c) Hirsch, R.; Katz, E.; Willner, I. *J. Am. Chem. Soc.* **2000**, *122*, 12053−12054.

(10) Katz, E.; Sheeney-Haj-Ichia, L.; Basnar, B.; Felner, I.; Willner, I. *Langmuir* **2004**, *20*, 9714−9719.

(11) Katz, E.; Baron, R.; Willner, I. *J. Am. Chem. Soc.* **2005**, *127*, 4060−4070.

10.1021/ja0517771 CCC: $30.25

and bioelectrochemical reactions at the electrode surface.[10] Also, the mechanism of the electrochemical processes of redox species associated with the electrode could be changed from the mechanism characteristic for an aqueous environment to the mechanism typical to a nonaqueous medium in the presence of the hydrophobic thin film generated by the hydrophobic nanoparticles on the electrode surface.[11] In the present article, we describe a new effect of hydrophobic magnetic nanoparticles on biorecognition and biocatalytic processes of DNA on a solid support. The magnetically induced attraction of the hydrophobic magnetic nanoparticles to the interface functionalized with an oligonucleotide monolayer results in its isolation from soluble complementary DNA or enzymes catalyzing DNA transformations, thus inhibiting the hybridization, polymerization, or hydrolytic digestion of the DNA on the surface. The magnetically induced retraction of the hydrophobic magnetic nanoparticles removes the hydrophobic thin film associated with the interface, thus reactivating the biorecognition and biocatalytic reactions of the DNA on the solid support. Reversible attraction and retraction of the hydrophobic magnetic nanoparticles to and from the functional interface by means of an external magnet allows the cyclic inhibition and activation of the DNA reactions, respectively. The reversible magnetoswitchable activation and inhibition of the DNA reactions were performed on electrode surfaces and followed electrochemically in situ using chronocoulometry and Faradaic impedance spectroscopy. The possible use of the results obtained in this study for the magnetic field-controlled fabrication of DNA chips and for the long-term stabilization of DNA sensors is discussed.

Experimental Section

Chemicals and Materials. Oligonucleotides **1**−**3** were prepared by Sigma-Genosys, Inc. Thiolated oligonucleotides **1** and **3** were reduced with dithiothreitol (DTT) and purified on a Sephadex G-25 column prior to the modification of surfaces. Viral DNA M13mp18 phage vector, deoxyribonuclease I (DNase I; from bovine pancreas; EC 3.1.21.1), DNA polymerase I (Klenow fragment; from *Escherichia coli*; EC 2.7.7.7), 1-mercaptohexanol, undecanoic acid, hexaammineruthenium(III) chloride ($Ru(NH_3)_6^{3+}$), and all other chemicals were purchased from Sigma or Aldrich and used without further purification. Magnetic nanoparticles, Fe_3O_4 (average diameter ca. 5 nm and saturation magnetization at room temperature of ca. 36.4 emu g^{-1}),[10] coated with undecanoic acid shell were synthesized according to the published procedure with the difference that only a single capping layer was generated on the surface of the nanoparticles.[12] Ultrapure water from NANOpure Diamond (Barnstead) source was used throughout all the experiments.

Chemical Modification of Electrodes. A Au-coated (250-nm gold layer) glass plate (22 × 22 mm^2) (Analytical μ-Systems, Germany) was used as a working electrode. Prior to the modification, the Au surface was purified by treatment with a piranha solution consisting of 70% (v/v) concentrated sulfuric acid and 30% (v/v) hydrogen peroxide for 15 min and then thoroughly rinsed with water. (*Caution*: *piranha solution reacts violently with organic compounds and should be handled with extreme care.*) The plate was then soaked in concentrated nitric acid for 5 min and rinsed again with water. The Au surface was interacted with a solution of **1** or **3**, 0.5 O.D. in 0.2 M phosphate buffer, pH 7.4, for 12 h. The resulting plate was washed with the phosphate buffer, and then the **1**- or **3**-functionalized Au surface was treated with 1-mercaptohexanol, 1 mM in 0.1 M phosphate buffer, pH = 7.4, for 1 h. The resulting oligonucleotide/1-mercaptohexanol mixed monolayer-functionalized Au surface was treated with **2** (5×10^{-7} M) or with the viral nucleic acid M13mp18 (1.7×10^{-9} M) in a solution composed of 10 mM phosphate buffer, pH = 7.4, and NaCl, 0.3 M, to yield the double-stranded (ds)-DNA assembly on the surface. Polymerization reaction on the M13mp18/**3**-assembly was performed in the presence of the dNTP mixture (dATP, dTTP, dCTP, and dGTP, 0.2 mM each) in a solution containing 20 mM Tris-HCl buffer, pH = 7.4, 10 mM $MgCl_2$, 60 mM KCL, and 0.1 units·μL^{-1} polymerase Klenow fragment. The resulting surface was then subjected to hydrolytic digestion catalyzed by DNase I in a solution composed of 10 mM Tris-HCl buffer, pH = 7.6, 2.5 mM $MgCl_2$, 0.5 mM $CaCl_2$, and 10 units·μL^{-1} DNase I. The DNA reactions were performed at ambient temperature (25 ± 2 °C).

Electrochemical Measurements. Chronocoulometry and Faradaic impedance spectroscopy were performed using an electrochemical analyzer (Autolab PGSTAT12, Eco Chemie B. V.). The measurements were carried out at ambient temperature (25 ± 2 °C) in a conventional electrochemical cell consisting of the modified Au electrode as a working electrode (0.78 cm^2 area exposed to the solution, roughness factor ca. 1.2), assembled at the bottom of the electrochemical cell, a glassy carbon auxiliary electrode, and a saturated calomel electrode (SCE) connected to the working volume with a Luggin capillary. All potentials are reported with respect to this reference electrode. Argon bubbling was used to remove oxygen from the solutions in the electrochemical cell. The cell was placed in a grounded Faraday cage. The electrochemical measurements were performed in the presence of soluble components required for the respective DNA reactions and an appropriate redox probe. Chronocoulometry measurements were performed in situ in the presence of $Ru(NH_3)_6^{3+}$, 50 μM, as a redox probe, by applying a potential step from 0.1 to −0.4 V. The Faradaic impedance measurements were performed in the presence of $K_3[Fe(CN)_6]/K_4[Fe(CN)_6]$, 1:1, mixture, 10 mM, as a redox probe. The Faradaic impedance spectra were recorded while applying a bias potential that equals the redox probe formal potential, 0.17 V, and using a 5 mV alternative voltage in the frequency range of 100 mHz to 10 kHz. The Faradaic impedance spectra were plotted in the form of complex plane diagrams (Nyquist plots). The experimental impedance spectra were fitted using electronic equivalent circuits to derive the electron-transfer resistance, R_{et}, values. For this purpose, commercial software (ZView, version 2.1b, Scribner Associates, Inc.) was employed.

The undecanoic acid-functionalized magnetic nanoparticles were added to the cell in a toluene solution (0.5 mL, 1 mg·mL^{-1}), yielding an upper organic solution layer immiscible with the aqueous electrolyte solution (2 mL). The undecanoic acid-functionalized magnetic nanoparticles were attracted to the Au electrode surface from the upper organic layer by positioning a 12-mm-diameter magnet (NdFeB/Zn-coated magnet with the remanent magnetization of 10.8 kG) below the bottom-working electrode. The magnetic nanoparticles were removed from the electrode surface and retransported to the organic phase by positioning the external magnet on top of the electrochemical cell.

Results and Discussion

The interfacial biorecognition or biocatalytic processes on the nucleic acid-functionalized supports include two kinds of the reacting components: The surface-confined nucleic acid units and the aqueous-phase-soluble complementary nucleic acids, or catalytically active enzymes. The recognition and binding of the soluble complementary DNA units to the nucleic acid-functionalized surface results in the increase of the DNA content on the interface. Alternatively, soluble enzymes can catalyze reactions for in the buildup or degradation of the DNA on the interface, resulting in the increase or decrease of its amount on the surface, respectively. All these processes require the contact of the biomolecule-functionalized surface with the

(12) Shen, L.; Laibinis, P. E.; Hatton, T. A. *Langmuir* **1999**, *15*, 447−453.

Scheme 1. Biorecognition and Biocatalytic Reactions of DNA on Electrode Surfaces[a]

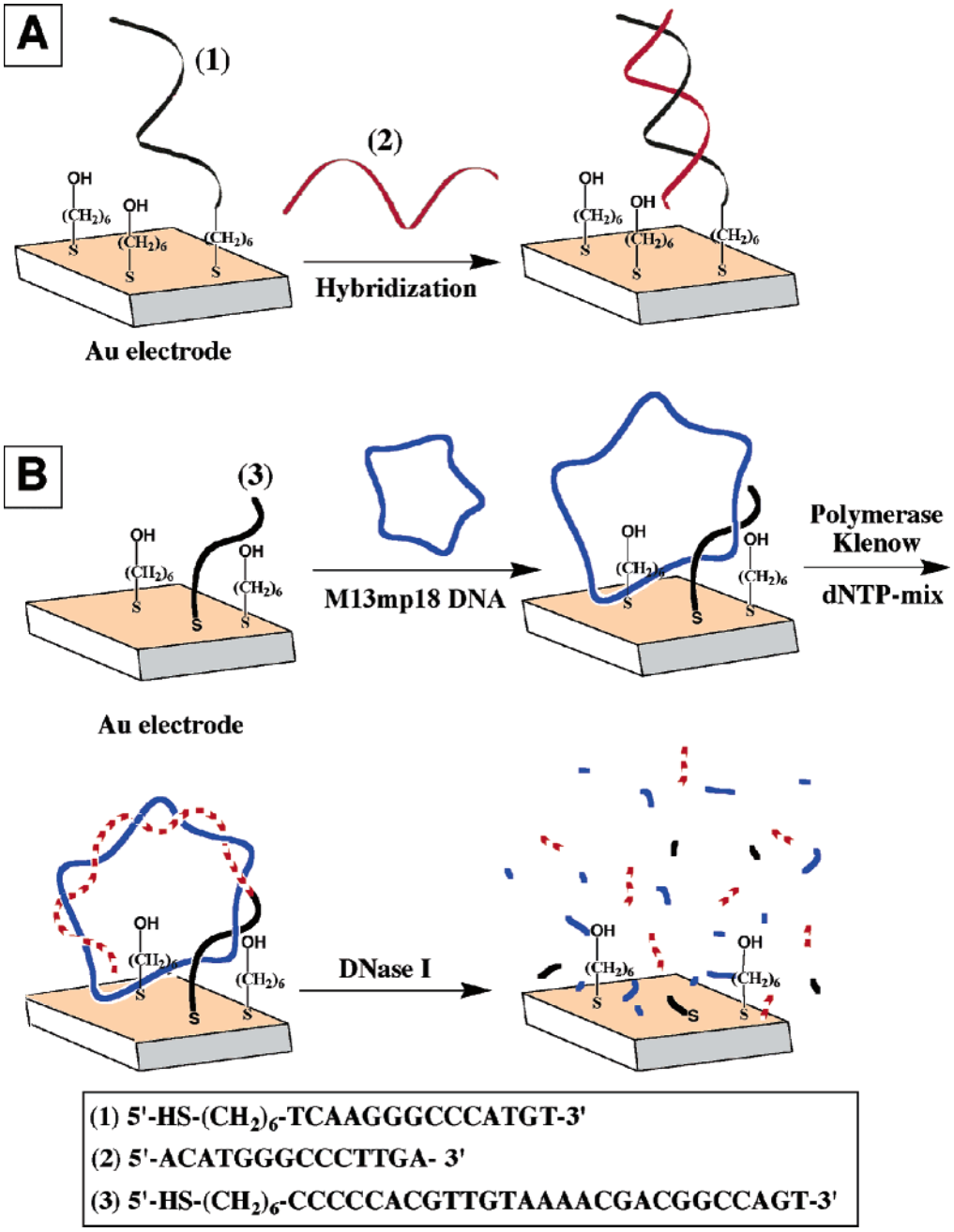

[a] (A) Hybridization of short oligonucleotides. (B) Hybridization, polymerization, and hydrolytic digestion of the long-chain viral DNA M13mp18 phage vector.

biomolecule-containing aqueous solution. It was recently shown[10,11] that the magnetically induced attraction of hydrophobic magnetic nanoparticles that carry associated nonaqueous solvent molecules to an electrode surface yields on an electrode a hydrophobic thin film that is nonpermeable for components solubilized in the aqueous electrolyte solution, thus generating a barrier for electrochemical and bioelectrochemical reactions. The hydrophobic thin film can be deposited on, or removed from, the electrode surface reversibly, thus resulting in the cyclic inhibition or activation of the electrochemical processes, respectively. One could expect that interfacial biorecognition and biocatalytic processes could be also inhibited and activated reversibly, in a similar manner. To verify this concept experimentally, we performed DNA hybridization, polymerization, and hydrolytic digestion on nucleic acid-modified electrode surfaces, while following the transformations at the surfaces by in situ electrochemical measurements. The biorecognition and biocatalytic processes were reversibly blocked and then activated upon attraction to and retraction from the electrode surface hydrophobic magnetic nanoparticles, respectively.

Magnetoswitchable Hybridization of DNA. Two different DNA systems were employed in this study: (i) a short oligonucleotide was hybridized with a nucleic acid-functionalized electrode surface and (ii) a long-chain viral DNA M13mp18 phage vector was hybridized with a complementary oligonucleotide-functionalized electrode surface. The formed DNA assembly was then subjected to the biocatalyzed polymerization in the presence of polymerase/dNTPs, and the resulting repli-

Scheme 2. Reversible Activation (A) and Inhibition (B) of the DNA Hybridization on the Electrode Surface by the Retraction from the Surface and Attraction to the Surface of the Hydrophobic Magnetic Nanoparticles, Respectively

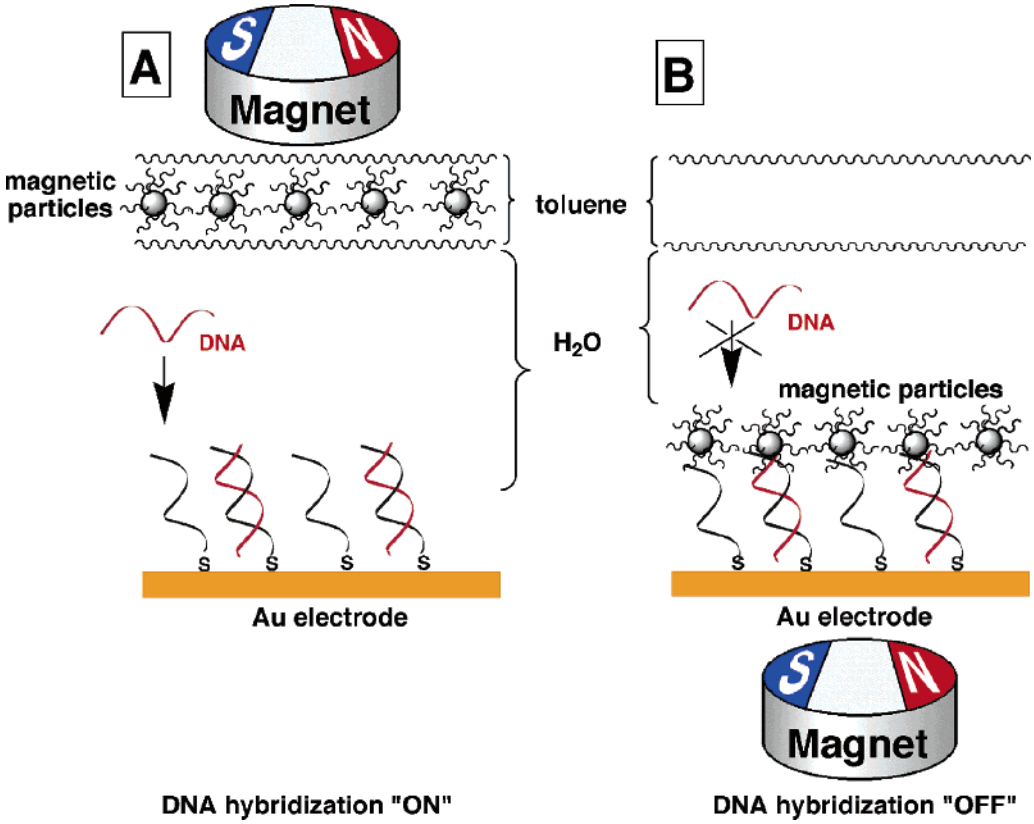

cated double-stranded DNA was then subjected to hydrolytic digestion in the presence of DNase I.

The first system that was studied involved the hybridization between the surface-confined oligonucleotide **1** and the complementary oligonucleotide **2**, 5×10^{-7} M, added to the aqueous solution (2 mL, 10 mM phosphate buffer, pH = 7.4, with NaCl, 0.3 M, and $Ru(NH_3)_6^{3+}$ redox probe, 50 μM; Scheme 1A). The **1**-functionalized Au electrode surface was treated prior to the hybridization with 1-mercaptohexanol to block pinholes in the DNA monolayer assembly associated with the electrode. The hydrophobic magnetic nanoparticles were dissolved in toluene (0.5 mL, 1 mg·mL^{-1}) to yield a magnetic fluid.[13] The toluene suspension of the magnetic nanoparticles was added to the electrochemical cell that included the aqueous solution to generate a biphase system consisting of two immiscible solutions. As the organic phase is lighter than the aqueous phase, the toluene solution is not in contact with the electrode surface that is located at the bottom of the electrochemical cell, thus allowing the hybridization process (Scheme 2A). The surface density of the single-stranded (ss)-DNA **1** prior to the hybridization process and the time-dependent increase of the DNA loading due to the formation of the ds-DNA **1**/**2** were derived from in situ chronocoulometry measurements in the presence of $Ru(NH_3)_6^{3+}$ as redox probe, $E° = -0.15$ V. For this purpose the $Ru(NH_3)_6^{3+}$ redox probe, 50 μM, was co-added to the aqueous solution. It is known that $Ru(NH_3)_6^{3+}$ cations serve as counter-ions that compensate the negative charge of oligonucleotides, thus allowing the quantitative analysis of the surface-confined DNA.[14] The electrochemical analysis of the redox probe associated with a DNA monolayer is performed in the presence of excess of the $Ru(NH_3)_6^{3+}$ in the background electrolyte to maintain the equilibrium of the charge-compensating cations bound to DNA. To separate the electrochemical response of the redox probe associated with the DNA monolayer from the response of the diffusional $Ru(NH_3)_6^{3+}$ species, the chronocoulometry technique was employed, and the surface loading of the redox probe, $\Gamma_{Ru-complex}$, was calculated using eq 1:[14]

$$Q = 2nFAD^{1/2}C\pi^{-1/2}t^{1/2} + Q_{dl} + nFA\Gamma_{Ru-complex} \quad (1)$$

where Q is the transient charge measured in the chronocoulometry experiment, $n = 1$ is the number of electrons per $Ru(NH_3)_6^{3+}$ ion involved in the electrochemical reduction process, F is the Faraday constant (C·equiv^{-1}), A is the electrode area (cm^2), D is the diffusion coefficient of $Ru(NH_3)_6^{3+}$ (cm^2·s^{-1}), C is the bulk concentration of $Ru(NH_3)_6^{3+}$ (mol·cm^{-3}), Q_{dl} is the capacitance charge (C), and $nFA\Gamma_{Ru-complex}$ is the charge associated with the reduction of $Ru(NH_3)_6^{3+}$ bound to the DNA monolayer. Figure 1A shows the chronocoulometric transients of the **1**-functionalized Au electrode in the absence and presence of $Ru(NH_3)_6^{3+}$, curves (a) and (b), respectively, upon applying a potential step from 0.1 to -0.4 V. The capacitance charge, Q_{dl}, was derived from the chronocoulometric transient measurement in the absence of the redox probe by the extrapolation of

(13) (a) Berkovsky, B. M.; Medvedev, V. F.; Karkov, M. S. *Magnetic Fluids: Engineering Applications*; Oxford University Press: New York, 1993. (b) Rosensweig, R. R. *Ferrohydrodynamics*; Cambridge University Press: Cambridge, England, 1985.

(14) Steel, A. B.; Herne, T. M.; Tarlov, M. J. *Anal. Chem.* **1998**, *70*, 4670−4677.

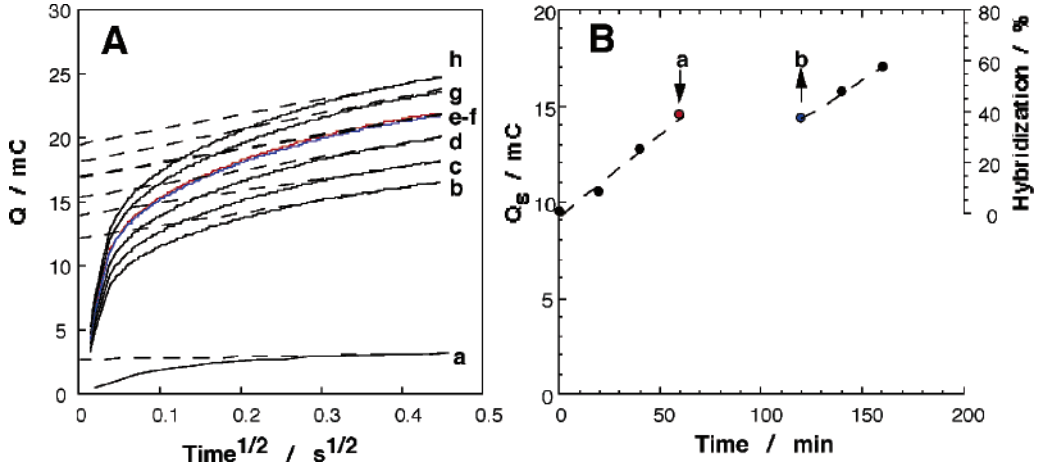

Figure 1. (A) Chronocoulometry transients recorded upon the application of a potential step from 0.1 to −0.4 V on the **1**-monolayer-functionalized Au electrode prior to hybridization in the absence of the redox probe, curve (a), and with the $Ru(NH_3)_6^{3+}$ redox probe, 50 μM, curve (b). Curves (c−e) during the hybridization with **2**, 5×10^{-7} M, at time intervals of 20 min; (f) immediately after the magnetic nanoparticles were removed from the electrode surface after they were attracted for 1 h, (g and h) during the reactivated hybridization at time intervals of 20 min. The data were recorded in 10 mM phosphate buffer, pH = 7.4, with NaCl, 0.3 M, under Ar. (B) Time-dependent charge corresponding to the reduction of the $Ru(NH_3)_6^{3+}$ redox probe associated with the surface-confined DNA (left scale) and the percentage of the hybridized DNA on the surface (right scale) derived from the chronocoulometry transients upon the hybridization process.

its linear part to $t = 0$ (Figure 1A, curve (a)). The sum of Q_{dl} and $nFA\Gamma_{Ru-complex}$ was derived from the chronocoulometric transient in the presence of the redox probe by the extrapolation of the linear part of curve (b) to $t = 0$. Thus, knowing Q_{dl}, the surface coverage of the DNA-bound $Ru(NH_3)_6^{3+}$, $\Gamma_{Ru-complex}$, was calculated to be 9.9×10^{-11} mol·cm^{-2}. Assuming that one $Ru(NH_3)_6^{3+}$ cation is linked to three DNA bases to compensate their charge,[14] and taking into account that the ss-DNA primer (**1**) contains 14 bases, the surface coverage of **1** corresponds to 2.1×10^{-11} mol·cm^{-2}. The amount of the DNA bases associated with the electrode surface increases upon the hybridization of the surface-confined DNA primer **1** with the complementary oligonucleotide **2** added to the aqueous solution. The increase of the content of DNA associated with the electrode as a result of the hybridization process was similarly followed by chronocoulometry, performing the measurements at time intervals of 20 min (Figure 1A, curves (c−e)). Figure 1B, left scale, shows the increase of the charge associated with the reduction process of the redox probe bound to the DNA that originates from the increase of the DNA content on the surface as a result of the hybridization process. Then, after 60 min of the hybridization process, an external magnet was placed below the electrochemical cell (point "a" in Figure 1B). The hydrophobic magnetic nanoparticles with the associated toluene molecules were attracted to the bottom electrode, resulting in the formation of the impermeable hydrophobic thin film on the electrode surface that inhibits further hybridization (Scheme 2B). In a previous study,[11] we revealed that the thin film has a thickness of ca. 8.5 μm and is composed of ca. 99% of the magnetic nanoparticles loaded into the system, while each nanoparticle is associated with ca. 410 molecules of toluene. After 1 h, the external magnet was placed above the electrochemical cell, resulting in the removal of the isolating thin film consisting of the magnetic nanoparticles and associated toluene, and their retranslocation to the top toluene phase. Immediately after the isolating thin film was removed from the electrode surface, the chronocoulometry transient was recorded, indicating that no changes of the DNA loading on the electrode surface had occurred during the time interval when the surface was isolated by the hydrophobic magnetic particles (Figure 1A, curve (f)). Thus, the hybridization process of the surface-confined **1** with the soluble complementary **2** was totally inhibited by the hydrophobic thin film. After the removal of the magnetic nanoparticles from the electrode support (point "b" in Figure 1B), the content of DNA linked to the electrode increased (Figure 1A, curves (g and h)), implying that hybridization of **2** with the **1**-functionalized interface was reactivated. This fact suggests that the inhibition of the hybridization by the magnetically deposited hydrophobic thin film is reversible, and the process can be reactivated by the removal of the magnetic nanoparticles from the surface (Figure 1B, left scale). The charge associated with the surface-confined redox probe was translated to the DNA surface loading, thus allowing us to derive the percent of the hybridized DNA on the surface (Figure 1B, right scale). The process starts from 0% of the hybridized DNA (only ss-DNA **1** exists on the surface). The amount of ds-DNA **1**/**2** increases when the electrode surface is exposed to the aqueous solution of **2**, and the process is interrupted when the hydrophobic isolating thin film is magnetically attracted to the surface.

Biorecognition and biocatalytic processes proceeding on an electrode surface result in the changes of interfacial properties that are reflected by the alteration of the double-layer capacitance and electron-transfer resistance. These changes can be followed by the Faradaic impedance spectroscopy.[15] Specifically, hybridization of DNA results in the increase of the negative charge on the interface, leading to higher electron-transfer resistance in the presence of a negatively charged soluble redox probe, for example, $[Fe(CN)_6]^{3-/4-}$. Indeed, Faradaic impedance measurements were used to follow hybridization of DNA on surfaces and biocatalytic transformations on surface-immobilized DNA.[15] It should be noted, however, that these measurements were never performed in situ. In the present study, we performed Faradaic impedance spectroscopy measurements to follow in situ the hybridization process outlined in Scheme 1A and to demonstrate the reversible inhibition and activation of this

(15) Katz, E.; Willner, I. *Electroanalysis* **2003**, *15*, 913−947.

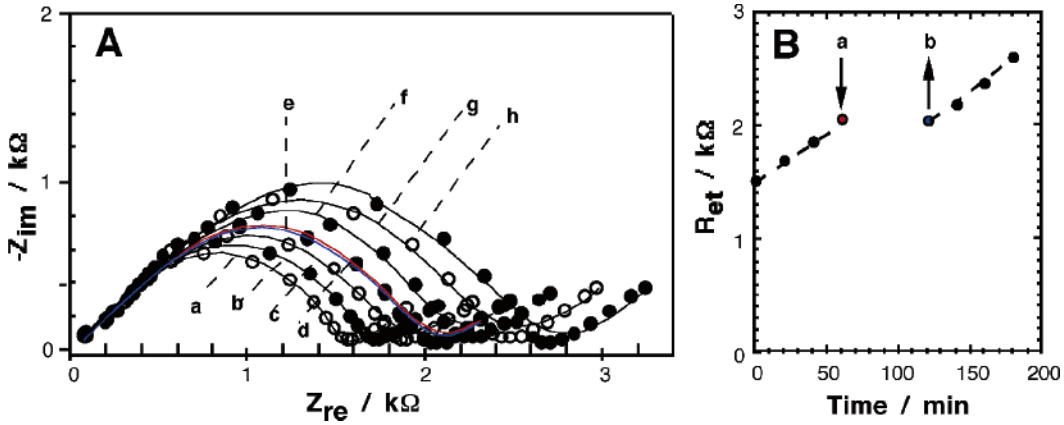

Figure 2. (A) Nyquist plots (Z_{im} vs Z_{re}) for the Faradaic impedance measurements performed on the **1**-monolayer-functionalized Au prior to and upon the hybridization process with **2**, 5×10^{-7} M: (a) prior to the hybridization, (b−d) during the hybridization at time-intervals of 20 min, (e) immediately after the magnetic nanoparticles were removed from the electrode surface after they were attracted for 1 h, (f−h) during the reactivated hybridization at time intervals of 20 min. The data were recorded in 10 mM phosphate buffer, pH = 7.4, with NaCl, 0.3 M, in the presence of 10 mM $K_3[Fe(CN)_6]/K_4[Fe(CN)_6]$, 1:1, bias potential of 0.17 V. (B) Time-dependent electron-transfer resistances derived from the experimental impedance spectra upon the hybridization process.

process by the attraction and removal of the hydrophobic magnetic nanoparticles to and from the electrode surface, respectively. In this experiment, the negatively charged redox probe $[Fe(CN)_6]^{3-/4-}$, 10 mM, was added to the aqueous solution instead of $Ru(NH_3)_6^{3+}$. Figure 2A shows the Faradaic impedance spectra of the system presented as Nyquist plots. Figure 2A, curve (a), shows the initial spectrum of the Au electrode modified with the primer oligonucleotide **1**. Then, the impedance spectra were recorded at time intervals of 20 min upon the hybridization process between the surface-confined **1** and the soluble complementary **2**. Figure 2A, curves (b−d), demonstrates the increase of the semicircle parts of the spectra. The increase in the diameter of the semicircle domains is attributed to the increase in the interfacial electron-transfer resistance as hybridization proceeds. That is, as the content of DNA on the surface is higher, the electrostatic repulsion of the negatively charged redox probe $[Fe(CN)_6]^{3-/4-}$ is enhanced, resulting in higher electron-transfer resistances. Afterward, an external magnet was placed below the electrochemical cell, resulting in the attraction of the magnetic nanoparticles to the electrode surface and in the formation of the nonpermeable hydrophobic thin film on the surface (point "a" in Figure 2B. This film was maintained on the electrode surface for 1 h. The impedance spectrum recorded at this time (Figure 3) shows an extremely high electron-transfer resistance, $R_{et} = 22$ kΩ, reflected by a large diameter semicircle domain that originates from the isolation of the electrode from the aqueous electrolyte solution that includes the redox probe by the hydrophobic thin film.[10] The impedance spectrum recorded immediately after the magnetic nanoparticles were removed from the electrode surface (Figure 2A, curve (e), and point "b" in Figure 2B) is similar to that observed before the deposition of the magnetic nanoparticles on the surface, curve (d), implying that the hybridization process was effectively interrupted for 1 h by blocking the electrode surface with the hydrophobic thin film. The impedance spectra recorded after that, at time intervals of 20 min, show a further increase in the diameter of the semicircle domains, confirming that the content of DNA associated with the surface is increased due to the reactivation of the hybridization process.

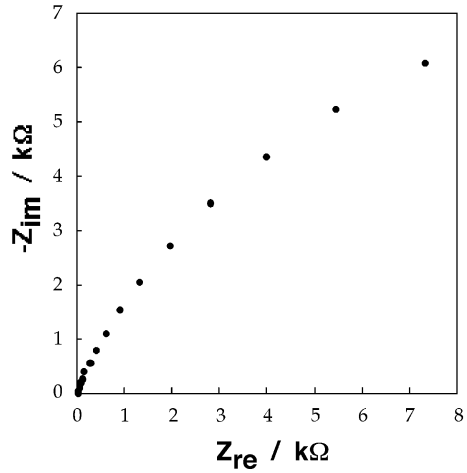

Figure 3. Nyquist plots (Z_{im} vs Z_{re}) for the Faradaic impedance measurements performed upon attraction of the hydrophobic magnetic nanoparticles to the DNA-functionalized Au electrode surface. The data were recorded in 10 mM phosphate buffer, pH = 7.4, with NaCl, 0.3 M, in the presence of 10 mM $K_3[Fe(CN)_6]/K_4[Fe(CN)_6]$, 1:1, bias potential of 0.17 V.

It should be noted that the electron-transfer resistance values, R_{et}, could be derived from the experimental impedance spectra as the diameters of the semicircle domains by fitting the impedance spectra to the equivalent electronic circuit based on the Randles and Ershler theoretical model (Scheme 3A).[16,17] This equivalent circuit includes the ohmic resistance of the electrolyte solution, R_s, the Warburg impedance, Z_W, resulting from the diffusion of the redox probe, the double-layer capacitance, C_{dl}, and the electron-transfer resistance, R_{et}. Two components of the circuit, C_{dl} and R_{et}, depend on the dielectric and insulating features of the electrode/electrolyte interface and are controlled by the surface modification of the electrode. In fact, the electron-transfer resistance, R_{et}, controls the interfacial electron-transfer rate between the redox probe in solution and the electrode support. It has been shown, however,[18] that the impedance

(16) (a) Bard, A. J.; Faulkner, L. R. *Electrochemical Methods: Fundamentals and Applications*; Wiley: New York, 1980. (b) Stoynov, Z. B.; Grafov, B. M.; Savova-Stoynova, B. S.; Elkin, V. V. *Electrochemical Impedance*; Nauka: Moscow, 1991.
(17) (a) Randles, J. E. B. *Discuss Faraday Soc.* **1947**, *1*, 11−19. (b) Ershler, B. V. *Discuss Faraday Soc.* **1947**, *1*, 269−277.
(18) Bardea, A.; Katz, E.; Willner, I. *Electroanalysis* **2000**, *12*, 1097−1106.

Scheme 3. Equivalent Electronic Circuits for Fitting of the Experimental Faradaic Impedance Spectra[a]

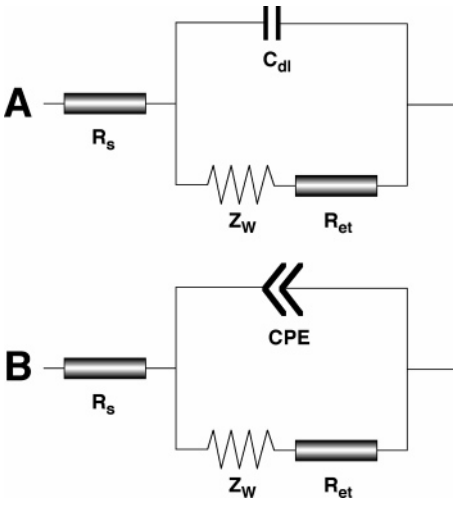

[a] (A) Circuit based on the Randles and Ershler theoretical model. (B) Circuit that includes a constant phase element (CPE) instead of the capacitance.

spectra of DNA-modified electrodes cannot be well fitted by this equivalent circuit and that an improved fit is obtained by substituting the capacitance with a constant phase element (CPE) in the equivalent circuit (Scheme 3B). The CPE reflects nonhomogeneity of the layer. The extent of the deviation from the Randles and Ershler model is controlled by the parameter n in eq 2, and the CPE becomes equal to the capacitance when $n = 1$.[15]

$$\mathrm{CPE} = A^{-1}(j\omega)^{-n} \tag{2}$$

The values of the parameter $n = 0.97 \pm 0.05$ were derived from the computer fitting of the experimental impedance spectra by the equivalent circuit that included CPE (Scheme 3B). Thus, the CPE in the equivalent circuit is almost equal to the capacitance, and the electron-transfer resistance values can be approximately derived from the diameters of the semicircle domains of the experimental impedance spectra. The exact values of R_{et} were determined by the computer fitting of the impedance spectra with the equivalent circuit that includes the CPE (Scheme 3B). Figure 2B shows the increase of the derived R_{et} upon the hybridization process and the unchanged R_{et} value during the time interval when the electrode surface was blocked by the hydrophobic thin film.

In the second part of the study, we modified the Au electrode surface with the thiolated 27-base oligonucleotide primer **3**, which is complementary to a domain of the natural single-stranded long-chain viral M13mp18 phage DNA vector that contains 7249 bases. The surface coverage of **3** was determined by microgravimetric quartz crystal microbalance experiments or chronocoulometry method to be 2.0×10^{-11} mol·cm^{-2}.[19] The **3**-functionalized Au electrode surface was also reacted with 1-mercaptohexanol to block pinholes in the DNA monolayer assembly associated with the electrode. The M13mp18 DNA, 1.7×10^{-9} M, was then added to the aqueous solution (2 mL, 10 mM phosphate buffer, pH = 7.4, with NaCl, 0.3 M), which also included $[Fe(CN)_6]^{3-/4-}$ redox probe, 10 mM, for the in situ Faradaic impedance measurements. In the first step of the experiment, M13mp18 DNA was hybridized with the **3**-functionalized Au surface (Scheme 1B), and the process was followed by the Faradaic impedance spectroscopy. Figure 4A, curves (a−e), shows the impedance spectra recorded at time intervals of 20 min upon the hybridization process. The increase in the diameters of the semicircle domains implies an increase in the interfacial electron-transfer resistance as hybridization proceeds. These results are consistent with the fact that hybridization elevates the content of the negatively charged DNA on the surface, thus enhancing the electrostatic repulsion of the negatively charged redox probe. Subsequently, the hydrophobic magnetic nanoparticles were attracted to the electrode surface by an external magnet placed below the electrochemical cell, and the electrode surface was blocked by the impermeable thin film (point "a" in Figure 4B). The Faradaic impedance spectrum, recorded when the electrode surface is blocked, shows a very high value of the electron-transfer resistance, reflected by a large semicircle domain (Figure 3). This is consistent with the formation of an insulating hydrophobic thin film on the electrode that blocks the electron transfer to the redox probe solubilized in the aqueous electrolyte solution. The magnetic nanoparticles were then removed from the electrode surface (by placing the external magnet above the cell) (point "b" in Figure 4B), and the impedance spectrum (Figure 4A, curve (f)) was found to be similar to that observed before the electrode blocking, curve (e). This fact suggests that the hybridization process of the soluble M13mp18 DNA with the **3**-functionalized Au surface was effectively inhibited by the deposition of the hydrophobic magnetic nanoparticles on the surface. The impedance spectra recorded at subsequent time intervals (Figure 4A, curves (g−j)) reveal an increase in the semicircle domains originating from the reactivation of the hybridization process. The electron-transfer resistance values were derived from the impedance spectra by the computer fitting with the equivalent circuit (Scheme 3B), and these are depicted in Figure 4B as a function of time. Clearly, the R_{et} values increase when the electrode surface is exposed to the aqueous solution that includes M13mp18 DNA, and the R_{et} value does not change during the time interval when the electrode surface is blocked by the hydrophobic thin film. Thus, the reversible inhibition and activation of the hybridization process on the electrode support by the attraction and retraction of the hydrophobic magnetic nanoparticles, respectively, was experimentally followed by the impedance spectroscopy using the electron-transfer resistance provided by the DNA layer as a readout signal. It should be noted, however, that the surface coverage of the long viral DNA cannot be quantitatively derived by chronocoulometry measurements, as it was performed for the short oligonucleotides **1**/**2**, since some of the redox probe units associated with the long DNA are sterically separated from the electrode surface and are not electrically contacted with the conductive support.

Magnetoswitchable Polymerization of DNA. The next step in the study involved the polymerization along the single-stranded part of M13mp18 DNA in the presence of the dNTP mixture and the enzyme polymerase Klenow fragment (Scheme 1B). The aqueous solution also included the $[Fe(CN)_6]^{3-/4-}$ redox probe, 10 mM, for the in situ Faradaic impedance analysis of the effect of the hydrophobic magnetic nanoparticles on the

(19) Patolsky, F.; Weizmann, Y.; Willner, I. *J. Am. Chem. Soc.* **2002**, *124*, 770−772.

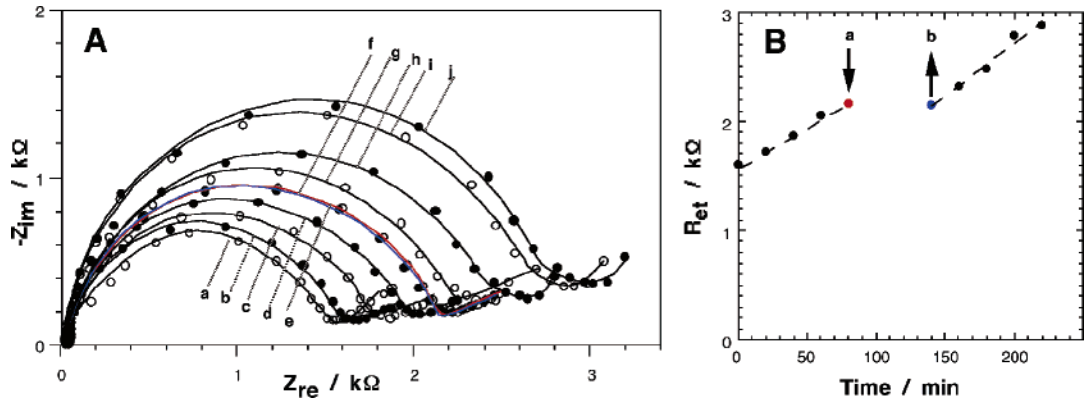

Figure 4. (A) Nyquist plots (Z_{im} vs Z_{re}) for the Faradaic impedance measurements performed on the **3**-monolayer-functionalized Au prior to and upon the hybridization process with M13mp18 DNA, 1.7×10^{-9} M: (a) prior to the hybridization, (b−e) during the hybridization at time intervals of 20 min, (e) immediately after the magnetic nanoparticles were removed from the electrode surface after they were attracted for 1 h, (f−j) during the reactivated hybridization at time intervals of 20 min. The data were recorded in 10 mM phosphate buffer, pH = 7.4, with NaCl, 0.3 M, in the presence of 10 mM $K_3[Fe(CN)_6]/K_4[Fe(CN)_6]$, 1:1, bias potential of 0.17 V. (B) Time-dependent electron-transfer resistances derived from the experimental impedance spectra upon the hybridization process.

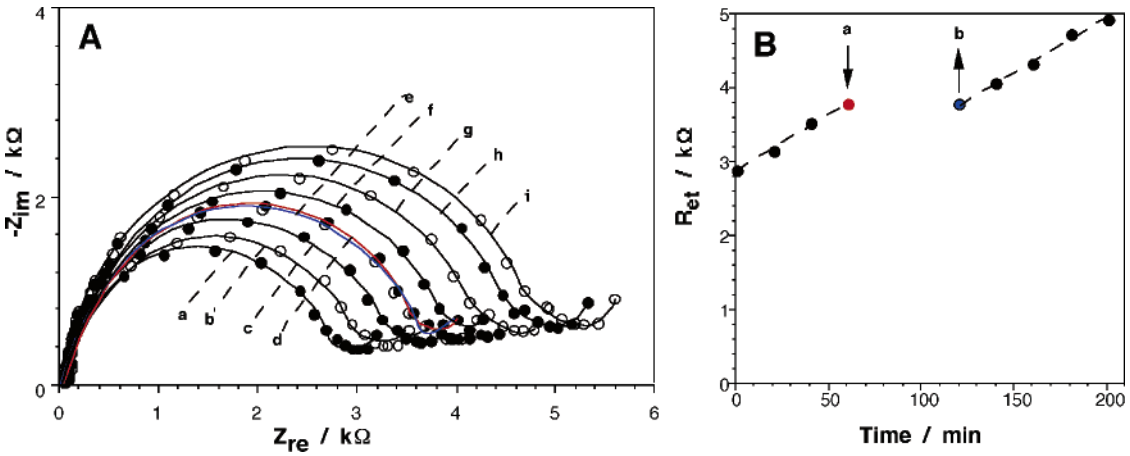

Figure 5. (A) Nyquist plots (Z_{im} vs Z_{re}) for the Faradaic impedance measurements performed on the **3**-monolayer-functionalized Au hybridized with M13mp18 DNA upon the polymerization process: (a) prior to the polymerization, (b−d) during the polymerization at time intervals of 20 min, (e) immediately after the magnetic nanoparticles were removed from the electrode surface after they were attracted for 1 h, (f−i) during the reactivated polymerization at time intervals of 20 min. The data were recorded in 20 mM Tris-buffer, pH = 7.4, containing $MgCl_2$, 60 mM, $K_3[Fe(CN)_6]/K_4[Fe(CN)_6]$, 1:1, 10 mM, the dNTP mixture (dATP, dTTP, dCTP, and dGTP, 0.2 mM each), and polymerase Klenow fragment, 0.1 units·μL^{-1}, bias potential of 0.17 V. (B) Time-dependent electron-transfer resistances derived from the experimental impedance spectra recorded upon the polymerization process.

polymerization process. Figure 5A, curves (a−d), shows the Faradaic impedance spectra recorded at time intervals of 20 min upon the polymerization process. The spectra show the increase of the semicircle domains, while polymerization proceeds. This originated from the increase of the DNA content associated with the electrode surface. The attraction of the hydrophobic magnetic nanoparticles to the surface by placing the external magnet below the electrochemical cell blocks the polymerization since the DNA-functionalized surface was isolated from the aqueous solution that contains the dNTP mixture and polymerase Klenow fragment (point "a" in Figure 5B). The impedance spectrum recorded immediately after the magnetic nanoparticles were removed from the surface (Figure 5A, curve (e) and point "b" in Figure 5B) is similar to that recorded just before the nanoparticles were attracted to the surface, curve (d), indicating that the amount of DNA was not changed during the time interval when the surface was blocked by the nanoparticles. At further 20 min time intervals, the impedance measurements reveal further increase of the semicircle domains in the spectra (Figure 5A, curves (f−i)). This implies that the polymerization process was reactivated upon the removal of the hydrophobic magnetic nanoparticles from the surface. The respective values of R_{et} were derived by fitting the experimental impedance spectra with the equivalent circuit (Scheme 3B). The R_{et} values plotted as a function of time (Figure 5B) reveal the increase of R_{et} before the electrode surface was blocked by the magnetic nanoparticles and the polymerization process proceeded, the unchanged R_{et} during the time interval when the surface was blocked by the nanoparticles, and the further increase of R_{et} when the magnetic nanoparticles were detracted from the surface and the polymerization was reactivated. Thus, the enzyme-catalyzed polymerization process of the surface-confined DNA assembly was reversibly inhibited and reactivated by the magnetically induced attraction and retraction of the nanoparticles to and from the electrode surface, respectively.

Magnetoswitchable Enzymatic Digestion of DNA. The last step of the study included the enzymatic digestion of the DNA assembly on the electrode in the presence of DNase I. The aqueous solution included DNase I and the $[Fe(CN)_6]^{3-/4-}$ redox probe, 10 mM, for the in situ Faradaic impedance spectroscopy. The biocatalyzed DNA digestion by DNase I was studied on the ds-DNA that was the polymerization product in the previous

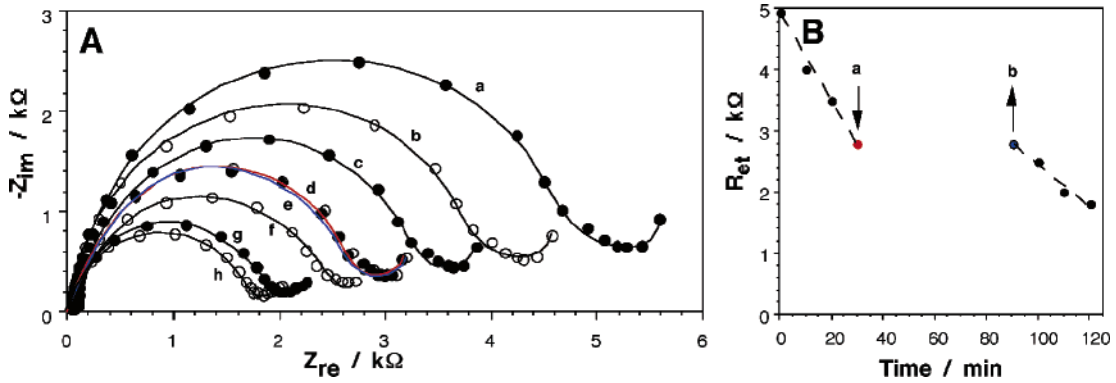

Figure 6. (A) Nyquist plots (Z_{im} vs Z_{re}) for the Faradaic impedance measurements performed on the **3**-monolayer-functionalized Au hybridized with M13mp18 DNA and further polymerized upon the hydrolytic digestion process: (a) prior to thehydrolytic digestion, (b−d) during the hydrolytic digestion at time intervals of 10 min, (e) immediately after the magnetic nanoparticles were removed from the electrode surface after they were attracted for 1 h, (f−h) during the reactivated hydrolytic digestion at time intervals of 10 min. The data were recorded in 10 mM Tris-HCl buffer, pH = 7.6, containing $MgCl_2$, 2.5 mM, $CaCl_2$, 0.5 mM, $K_3[Fe(CN)_6]/K_4[Fe(CN)_6]$, 1:1, 10 mM, and DNase I, 10 units·μL^{-1}, bias potential of 0.17 V. (B) Time-dependent electron-transfer resistances derived from the experimental impedance spectra recorded upon the hydrolytic digestion process.

system. The hydrolytic digestion of the ds-DNA is anticipated to decrease the amount of DNA on the electrode surface, thus leading to the decrease of the R_{et} values. Figure 6A, curves (a−d), shows the Faradaic impedance spectra recorded upon the hydrolytic digestion at time intervals of 10 min (the hydrolytic digestion is faster than the hybridization and polymerization processes, and thus the applied time intervals were shorter). Obviously, the semicircle domains of the spectra turn smaller while the hydrolytic digestion proceeds. This is consistent with the removal of the DNA content associated with the surface that results in lower electrostatic repulsion of the solubilized redox probe, thus leading to the decrease in the interfacial electron-transfer resistance. Subsequently, the hydrolytic digestion was interrupted by the attraction of the hydrophobic magnetic nanoparticles to the electrode surface (point "a" in Figure 6B). The impedance spectrum recorded immediately after the retraction of the nanoparticles from the surface (Figure 6A, curve (e)) was similar to that measured just before the hydrolytic digestion was blocked by the attraction of the nanoparticles to the surface, curve (d). After the hydrophobic magnetic nanoparticles were removed from the surface (point "b" in Figure 6B), the hydrolytic digestion was reactivated, and the recorded impedance spectra show a further decrease of the semicircle domains (Figure 6A, curves (f−h)). The respective R_{et} values were derived by fitting the experimental impedance spectra to the equivalent circuit (Scheme 3B), and the R_{et} values were plotted as a function of time (Figure 6B). The R_{et} values decreased upon the hydrolytic digestion, and R_{et} did not change when the process was inhibited by the attraction of the hydrophobic magnetic nanoparticles to the electrode surface. The inhibition was reversible, and the hydrolytic digestion was reactivated by the magnetically induced retraction of the nanoparticles from the electrode surface.

Conclusions

The attraction of hydrophobic magnetic nanoparticles to an electrode surface immersed in a water−toluene biphase system by means of an external magnetic field results in the formation of a hydrophobic thin film on the surface. The resulting interface is impermeable to species dissolved in the aqueous solution. In the present study, we examined the effect of the magnetically attracted nanoparticles to the electrode on the hybridization, polymerization, and hydrolytic digestion of DNA associated with the electrode surface. We found that the hydrophobic thin film generated by the magnetic nanoparticles blocks the surface-confined DNA layer from the water-soluble reactive species, such as the complementary DNA, thus preventing hybridization, or DNA-reactive enzymes (e.g., polymerase or DNase I), thus inhibiting the polymerization or hydrolytic digestion processes. Retraction of the hydrophobic magnetic nanoparticles from the electrode surface by the external magnetic field regenerates the DNA-functionalized electrode surface and reactivates the hybridization, polymerization, or hydrolytic digestion processes. Thus, the hydrophobic magnetic nanoparticles enable the reversible inhibition of the biorecognition and biocatalytic processes occurring on the DNA-functionalized surfaces. The hybridization process was followed in situ by chronocoulometry that allows us to derive the amount of the surface-associated DNA quantitatively. The hybridization, polymerization, or hydrolytic digestion processes were also followed in situ by Faradaic impedance spectroscopy that allows us to follow the interfacial properties (namely electron-transfer resistance, R_{et}) upon the increase or decrease of the content of the surface-confined DNA as a result of hybridization, polymerization, or hydrolytic digestion. It should be noted that, to the best of our knowledge, these experiments represent the first successful attempt to follow in situ the hybridization, polymerization, and hydrolytic digestion of DNA associated with electrode supports.

One major aspect of this study relates to the possible applications of the magnetic field-induced reversible inhibition of DNA reactivity on surfaces by means of the hydrophobic magnetic nanoparticles. We may see two major applications of these results. (i) One possible benefit relates to the stabilization and storage of DNA/RNA sensing surfaces. The degradation of functional interfaces by microbial digestion is anticipated to be blocked by protecting the surfaces with the hydrophobic magnetic nanoparticles attracted to the surfaces by means of an external magnet, thus leading to the enhanced stabilization of the sensing interfaces during their storage. (ii) Even more exciting promise rests on the possible use of the results to generate DNA (or eventually peptide) arrays on chips. The photochemically induced fabrication of DNA chips by selective exposure of a specific surface domain that deprotects a photo-

labile group and enables site-selective synthesis is the basis to generate DNA (or peptide) arrays on surfaces.[20] To date, there are technologies to generate microscale circuitry that enable the generation of localized magnetic fields by passage of current.[21] The use of such magnetic circuit patterns would allow the selective and controlled exposure of surface domains for sequential synthesis and would result in a new method for the fabrication of biochips.

Acknowledgment. This research is supported by the EC MOLDYNLOGIC project.

JA0517771

(20) Young, R. A. *Cell* **2000**, *102*, 9−15.
(21) (a) Lee, C. S.; Lee, H.; Westervelt, R. M. *Appl. Phys. Lett.* **2001**, *79*, 3308−3310. (b) Lee, H.; Purdon, A. M.; Chu, V.; Westervelt, R. M. *Nano Lett.* **2004**, *4*, 995−998.